

g_mmpbsa - A GROMACS tool for high-throughput MM-PBSA Calculations

Rashmi Kumari¹, Rajendra Kumar¹, OSDD Consortium² and Andrew Lynn^{1}*

¹ School of Computational and Integrative Sciences, Jawaharlal Nehru University, New Delhi, 110067, India.

² CSIR Open Source Drug Discovery Unit, Anusandhan Bhavan, 2 Rafi Marg, New Delhi 110001, India.

Supporting Information

Contents

Table S1	3
Table S2	4
Table S3	11
Table S4	12
Figure S1	13
Figure S2	14
Figure S3	15
Figure S4	16
Figure S5	17
Figure S6	18
Figure S7	19
Figure S8	20
Figure S9	21
References	22

TABLES

Table S1: Different sets of atomic radii implemented in *g_mmpbsa* tool. The atomtype for which radius is not given in the following table, it is simply the corresponding element radius. For example, radius for HC atomtype is similar to H atomtype in case of the bondi radii set.

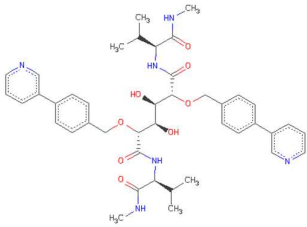
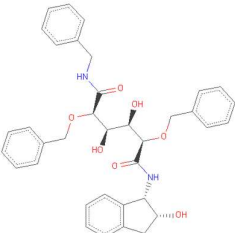
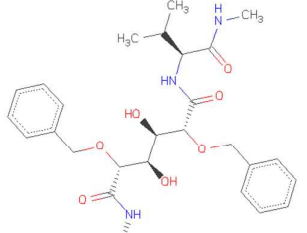
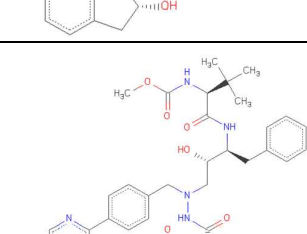
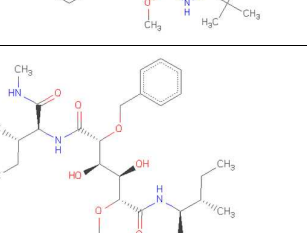
Atom Type	bondi* (Å)	mbondi# (Å)	mbondi2 [⊗] (Å)
O	1.52	1.50	1.50
S	1.83	1.80	1.80
N	1.55	1.55	1.55
C	1.70	1.70	1.70
H	1.20	1.20	1.20
P	1.80	1.85	1.85
F	1.47	1.47	1.47
I	2.06	1.98	1.98
Cl	1.77	1.77	1.77
Br	1.92	1.85	1.85
HC	–	1.30	1.30
CA	1.77	1.77	–
CB	1.77	1.77	–
CC	1.77	1.77	–
CN	1.77	1.77	–
CR	1.77	1.77	–
CV	1.77	1.77	–
CW	1.77	1.77	–
C*	1.77	1.77	–
CD	1.77	1.77	–
HA	1.00	1.00	–
H4	1.00	1.00	–
H5	1.00	1.00	–
HN	–	1.30	1.30
HO	–	0.80	0.80
HS	–	0.80	0.80
HP	–	1.30	1.30

* From reference¹

From reference² and¹

⊗ From reference²⁻⁴ and¹

Table S2: Chemical structures of the 37 HIV-1 protease inhibitor complexes taken for the binding energy calculation and their experimental inhibition constants K_i (nM).

S. No.	PDB ID	K_i (nM)	Protonation ASP-Chain ID	Ligand PDB Code	Ligand Structure
1	1EC2	0.1	ASP25-A	BEJ	 The chemical structure of BEJ is a complex molecule featuring a central core with multiple stereocenters. It includes a piperidine ring, a pyridine ring, and several amide and ester groups. The structure is highly branched and contains several hydroxyl groups.
2	1D4H	0.1	ASP25-A	BEH	 The chemical structure of BEH is a complex molecule with a central core and several stereocenters. It features a piperidine ring, a pyridine ring, and several amide and ester groups. The structure is highly branched and contains several hydroxyl groups.
3	1EBZ	0.4	ASP25-A	BEC	 The chemical structure of BEC is a complex molecule with a central core and several stereocenters. It features a piperidine ring, a pyridine ring, and several amide and ester groups. The structure is highly branched and contains several hydroxyl groups.
4	2AQU	0.48	ASP25-B	DR7	 The chemical structure of DR7 is a complex molecule with a central core and several stereocenters. It features a piperidine ring, a pyridine ring, and several amide and ester groups. The structure is highly branched and contains several hydroxyl groups.
5	1EBW	0.9	ASP25-A	BEI	 The chemical structure of BEI is a complex molecule with a central core and several stereocenters. It features a piperidine ring, a pyridine ring, and several amide and ester groups. The structure is highly branched and contains several hydroxyl groups.

6	1EC3	0.92	ASP125-B	MS3	
7	1EC1	1.2	ASP25-A	BEE	
8	1T7K	1.37	ASP25-B	BH0	
9	1D4I	1.4	ASP25-A	BEG	
10	2CEJ	2.4	ASP25-A	1AH	

11	1EC0	3.2	ASP125-B	BED	
12	2UXZ	3.3	ASP125-B	HI1	
13	1W5Y	3.3	ASP25-B	BE6	
14	1W5X	4	ASP25-B	BE5	
15	1D4J	4.4	ASP25-A	MSC	

16	2CEN	5	ASP25-A	4AH	
17	1W5V	7.1	ASP25-A	BE3	
18	1G35	7.3	ASP25-B	AHF	
19	2BQV	9	ASP125-B	A1A	
20	1G2K	11	ASP25-B	NM1	
21	2CEM	12	ASP25-A	2AH	

22	1AJX	12.2	ASP25-B	AH1	
23	1AJV	19.9	ASP25-B	NMB	
24	1IZH	20	ASP25-B	Q50	
25	2PSU	24	ASP25-A	MUU	
26	1XL5	45	ASP25-A	190	
27	2PSV	58	ASP25-A	MUV	

28	2QNN	70	ASP25-A	QN1	
29	2UY0	120	ASP25-A	HV1	
30	2PWR	260	ASP25-A	G4G	
31	2PWC	270	ASP25-A	G3G	
32	2QNP	390	ASP25-A	QN2	
33	2QNQ	770	ASP25-B	QN3	
34	3BGB	900	ASP25-B	LJG	

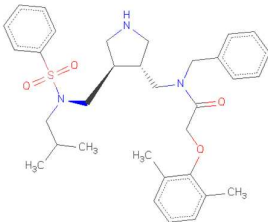
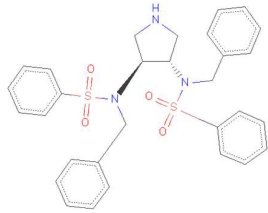
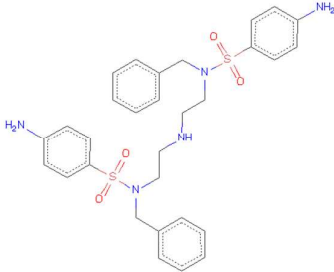
35	1XL2	1500	ASP25-B	189	
36	2PQZ	2150	ASP25-B	G0G	
37	3BGC	9600	ASP25-B	LJH	

Table S3: Comparison of the average binding energies (kJ/mol) obtained from the 800 and 17 snapshots using direct and the bootstrap analysis method, respectively. The autocorrelation time for each complex was calculated using *g_analyze* of GROMACS package. For G_{polar} , input parameters, bondi radii set, 0.5 Å grid resolution, $\epsilon_{solute} = 2$ and LPBE solver were used. For $G_{non-polar}$, SASA-only model was used.

Complex ID	Autocorrelation time (ps)	$\langle \Delta E \rangle$ ($n = 800$)	$\langle \Delta E_{bootstrap} \rangle$ ($n = 17$)	Std. Error (bootstrap)	$ \langle \Delta E \rangle - \langle \Delta E_{bootstrap} \rangle $
1EC2	54	-143.11	-144.61	3.19	1.50
1D4H	12	-171.15	-168.77	3.65	2.38
1EBZ	1	-203.41	-206.58	4.86	3.17
2AQU	105	-159.15	-160.19	5.57	1.04
1EBW	161	-152.56	-148.75	6.10	3.81
1EC3	201	-210.83	-212.79	6.27	1.96
1EC1	135	-186.67	-185.65	3.85	1.02
1T7K	10	-182.19	-178.60	2.92	3.59
1D4I	1	-202.45	-206.38	3.84	3.93
2CEJ	22	-174.32	-180.38	3.12	6.06
1EC0	79	-199.09	-195.45	5.50	3.64
2UXZ	444	-187.97	-184.92	6.25	3.05
1W5Y	38	-166.54	-164.22	3.36	2.32
1W5X	20	-208.70	-213.53	5.39	4.83
1D4J	2	-174.33	-176.91	5.43	2.58
2CEN	39	-156.49	-158.81	6.32	2.32
1W5V	37	-229.69	-231.45	3.32	1.76
1G35	51	-157.17	-153.70	3.57	3.47
2BQV	37	-148.83	-140.31	3.18	8.52
1G2K	21	-174.35	-172.17	4.14	2.18
2CEM	59	-161.96	-155.94	5.39	6.02
1AJX	274	-144.76	-150.97	3.75	6.21
1AJV	28	-161.93	-155.25	4.03	6.68
1IZH	16	-161.01	-161.17	5.00	0.16
2PSU	6	-130.55	-134.05	3.06	3.50
1XL5	26	-159.75	-161.71	3.78	1.96
2PSV	9	-106.69	-111.65	2.98	4.96
2QNN	21	2.34	10.83	5.40	8.49
2UY0	4	-167.61	-163.92	3.81	3.69
2PWR	76	10.51	11.28	3.52	0.77
2PWC	94	11.72	10.87	3.24	0.85
2QNP	23	-29.98	-32.08	3.63	2.10
2QNQ	24	-6.68	-5.91	3.68	0.77
3BGB	19	-16.80	-19.88	2.82	3.08
1XL2	110	-26.24	-30.90	3.84	4.66
2PQZ	25	9.01	5.07	3.95	3.94
3BGC	15	-37.64	-39.12	3.42	1.48

Table S4: List of the input parameters that were used to calculate polar-solvation energy using *g_mmpbsa* and *mmpbsa.pl* (AMBER package).

<i>g_mmpbsa</i> (APBS package)		<i>mmpbsa.pl</i> (PBSA of the AMBER suite)	
Parameter	Value	Parameter	Value
cfac	1.5	Not available	
gridspace	0.5	SCALE (grid-points/Angstrom)	2
fadd	5	Not Available	
gmemceil	5000	Not Available	
pconc	0	ISTRNG	0
nconc	0	ISTRNG	0
vdie	1	INDI	1
pide	1	INDI	1
sdie	80	EXDI	80
srad	1.4	PRBRAD	1.4
temp	300	Not Available	
srfm	smol	Not Available	
chgm	spl4	Not Available	
bcbf	mdh	Not Available	
PBSolver	lpbe	Not Available	
Not Available		LINIT (iterations with linear PB solver)	1000

FIGURES

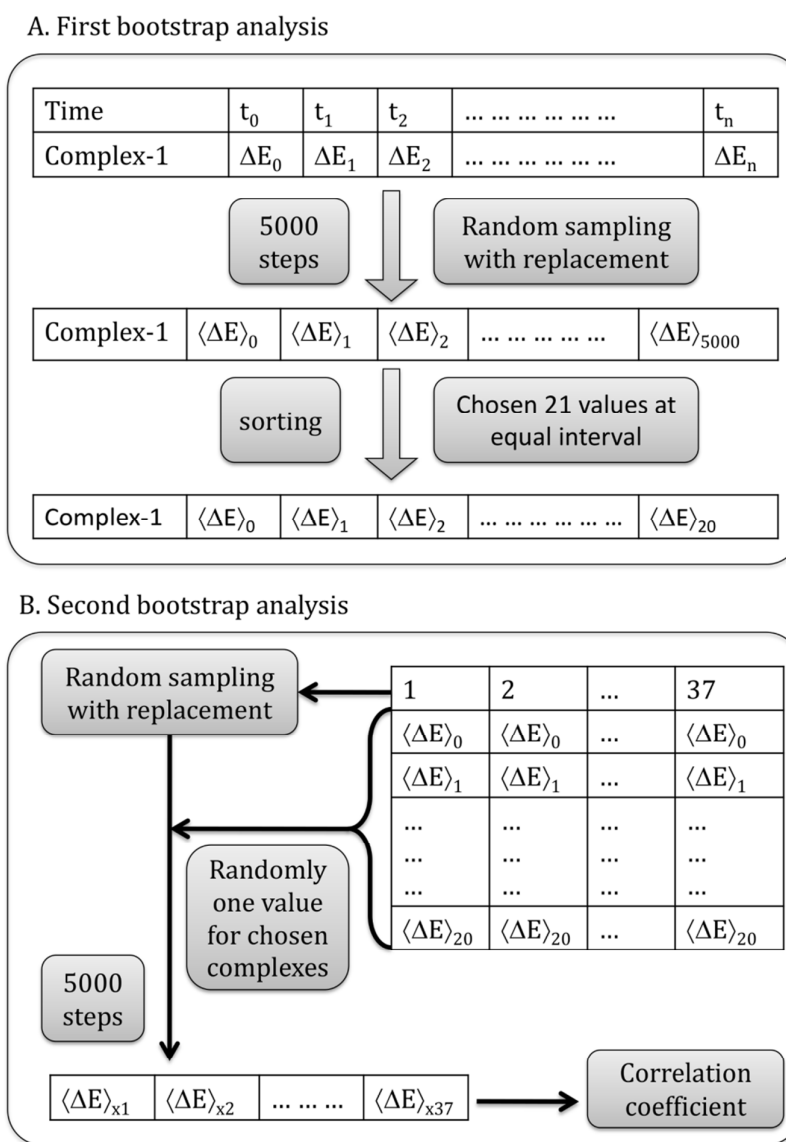


Figure S1: An overview of the procedure, which was used to calculate the correlation distribution and confidence interval using bootstrap analysis. (A) At first, 21 average binding energy values were obtained from 5000 bootstrap runs on 17 snapshots as illustrated in the flow-chart. This procedure was performed separately for all 37 complexes. (B) Subsequently, 21 energy values of the respective complex (shown in inset table) were used as a sampling group to calculate correlation coefficient during each step of the bootstrap. The 5000 correlation coefficients obtained from 5000 bootstrap steps were further used to calculate mean, mode and 99 % confidence interval.

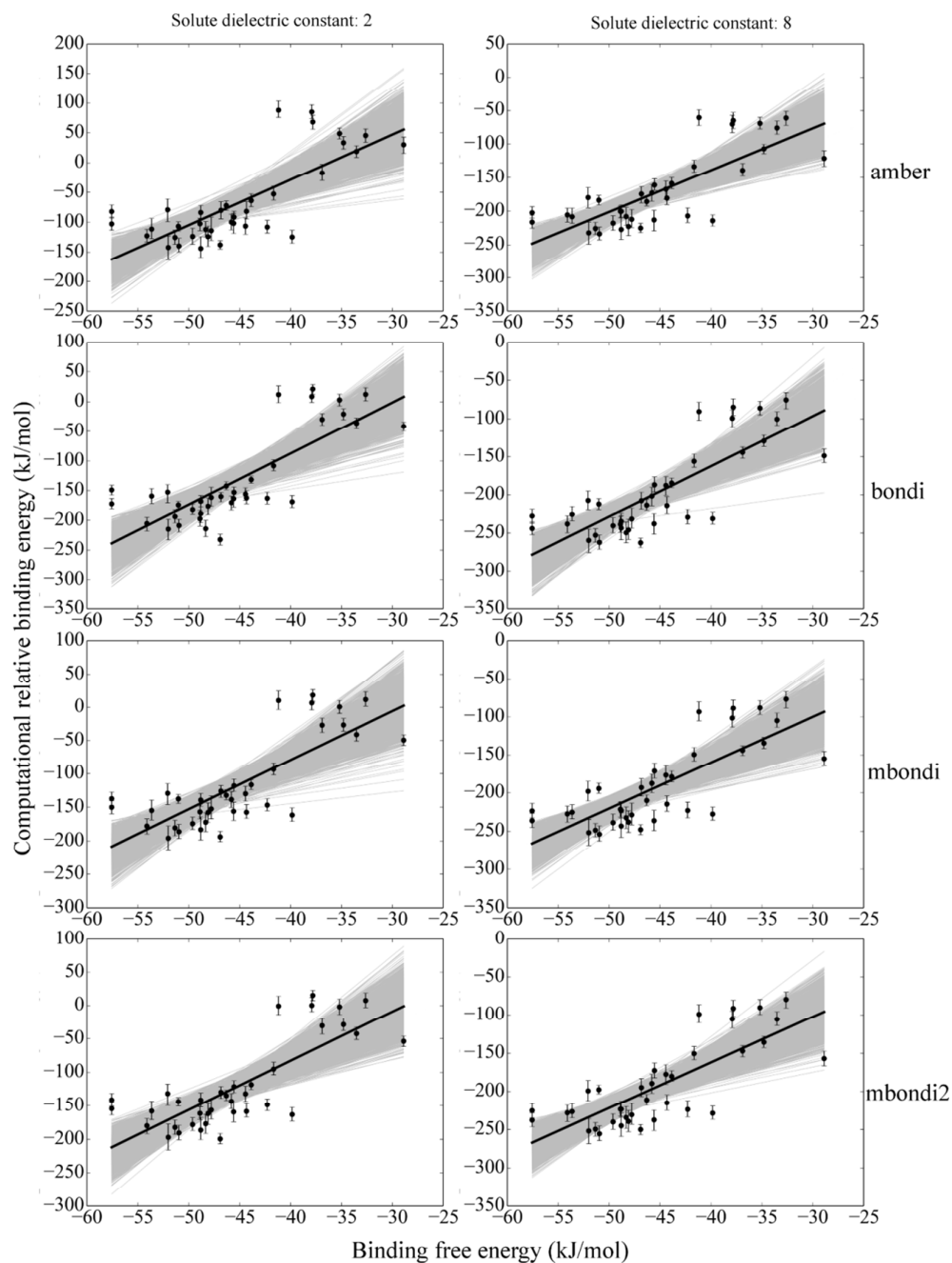


Figure S2: Correlation between experimental binding free energy and calculated binding energy (kJ/mol). The dots represent mean of average binding energy after bootstrap and the error bars are 99% confidence interval of mean distribution. Following are the parameters values/choices taken for the G_{polar} : Linear PBE, $\epsilon_{solute} = 2$ and grid resolution of 0.5 \AA (Left panel); Linear PBE, $\epsilon_{solute} = 8$ and grid resolution of 0.5 \AA (Right panel). SASA-only model has been taken for $G_{non-polar}$ calculation for each calculation.

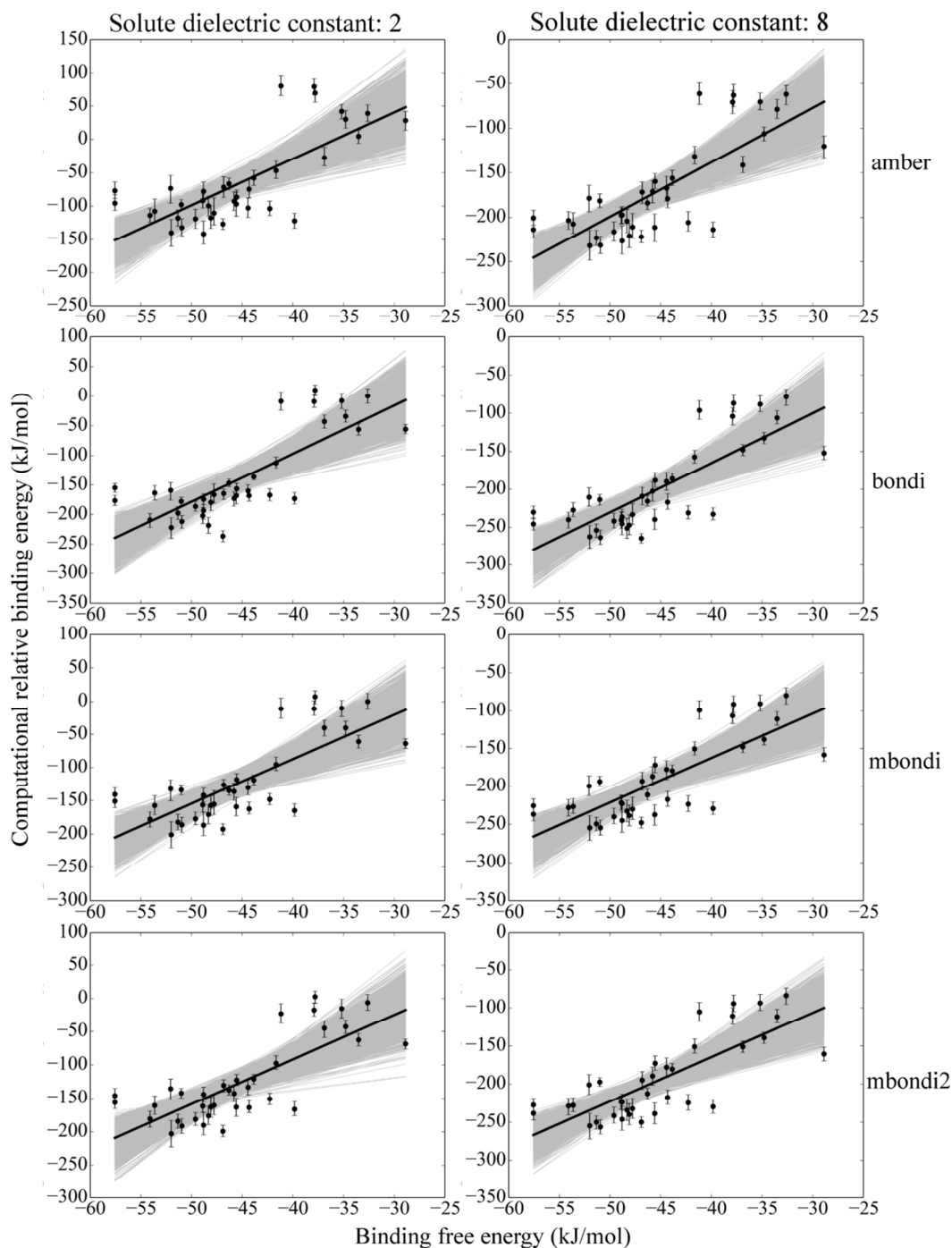


Figure S3: Correlation between experimental binding free energy and calculated binding energy (kJ/mol). The dots represent mean of average binding energy after bootstrap and the error bars are 99% confidence interval of mean distribution. Following are the parameters values/choices taken for the G_{polar} : Non-linear PBE, $\epsilon_{solute} = 2$ and grid resolution of 0.5 \AA . (Left panel); Non-linear PBE, $\epsilon_{solute} = 8$ and grid resolution of 0.5 \AA (Right panel). SASA-only model has been taken for $G_{non-polar}$ calculation for each calculation.

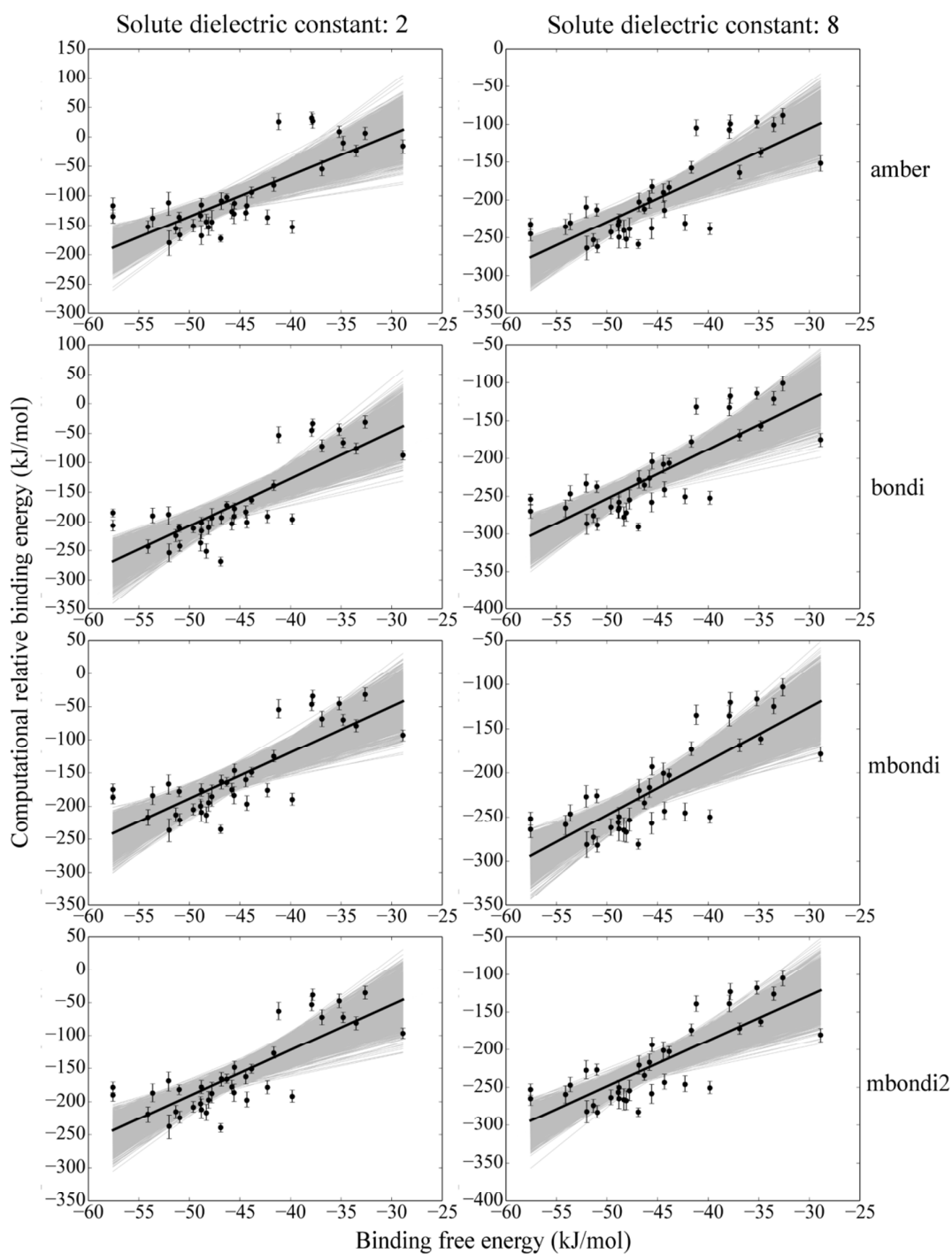


Figure S4: Correlation between experimental binding free energy and calculated binding energy (kJ/mol). The dots represent mean of average binding energy after bootstrap and the error bars are 99% confidence interval of mean distribution. Following are the parameters values/choices taken for the G_{polar} : Non-linear PBE, $\epsilon_{solute} = 2$ and grid resolution of 0.2 Å. (Left panel); Non-linear PBE, $\epsilon_{solute} = 8$ and grid resolution of 0.2 Å (Right panel). SASA-only model has been taken for $G_{non-polar}$ calculation for each calculation.

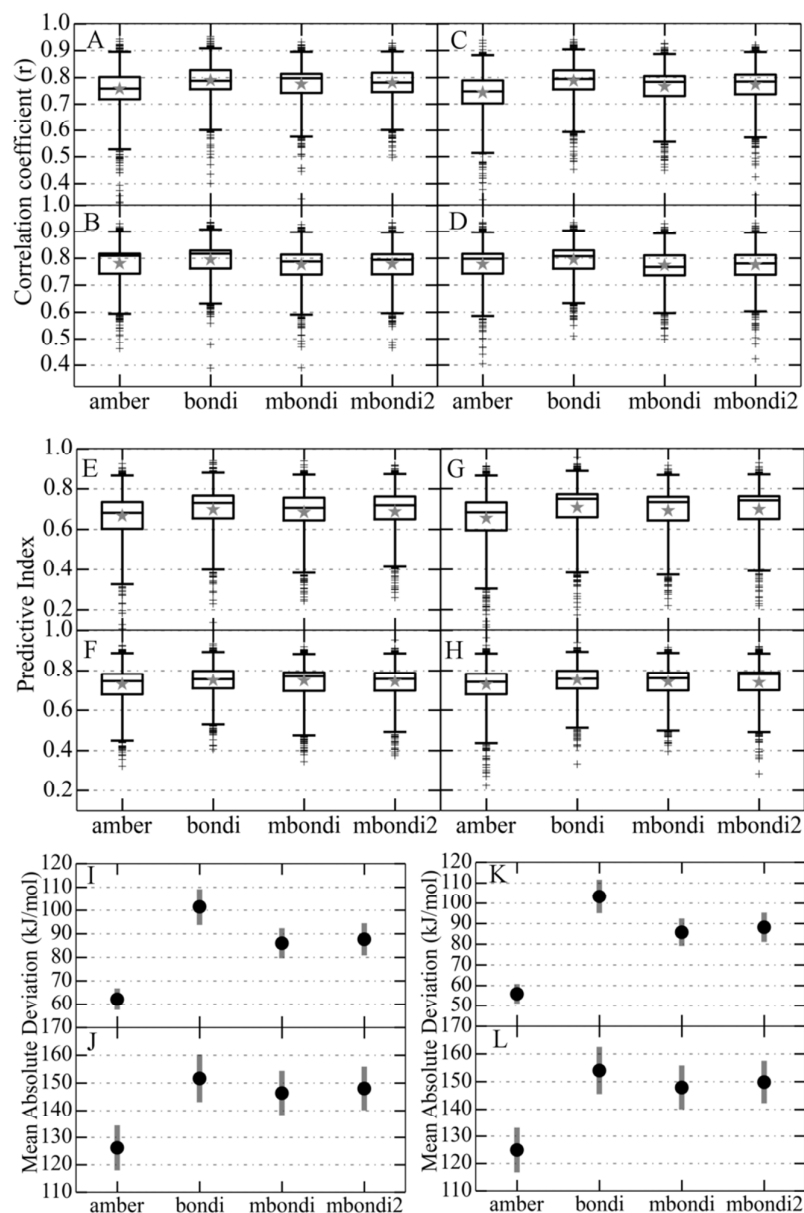


Figure S5: Influence of atomic radii, dielectric constant and PBE solver on the correlation. The predictive index (PI) and means absolute deviation (MAD) calculated for the same parameter combinations are also shown. (A-H) Box shows 50% region of the obtained distribution of the respective quantity (Y-axis label) from the bootstrap analysis. Horizontal line shown inside box depicts mode value of the distribution. Error-bar shows 99% region of the distribution. Symbols ('+') outside error-bar show remaining 1% of the distribution. The average correlation coefficient is shown by Asterisk symbol. (I-L) for the MAD: black dots and error-bar represent average value and standard error, which is calculated using the bootstrap analysis. Following are the parameters values/choices taken for the G_{polar} . (A,E,I) Linear PBE, $\epsilon_{solute} = 2$ and grid resolution of 0.5 Å. (B,F,J) Linear PBE, $\epsilon_{solute} = 8$ and grid resolution of 0.5 Å. (C,G,K) Non-linear PBE, $\epsilon_{solute} = 2$ and grid resolution of 0.5 Å. (D,H,L) Non-linear PBE, $\epsilon_{solute} = 8$ and grid resolution of 0.5 Å.

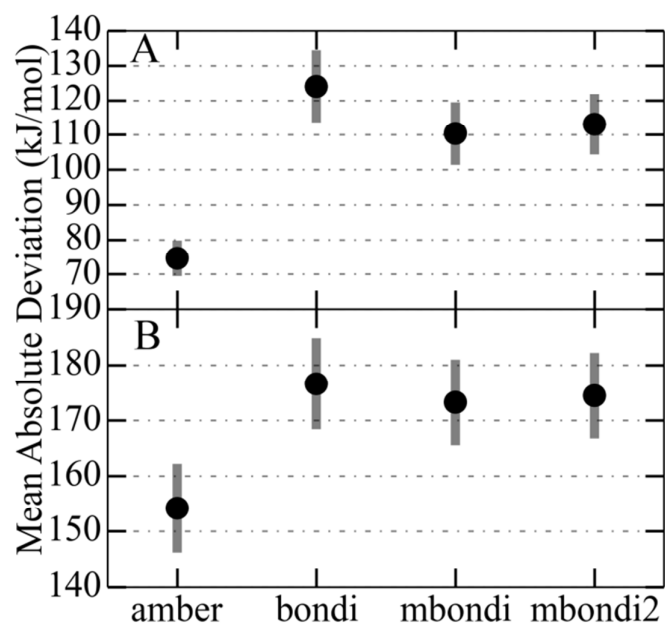


Figure S6: Mean absolute deviation (MAD) in the predicted energy using grid resolution 0.2 Å and NPBE solver. Black dots and error-bar represent average values and standard errors that were calculated using the bootstrap analysis. The obtained MAD values are shown for (A) $\epsilon_{solute} = 2$ and (B) $\epsilon_{solute} = 8$.

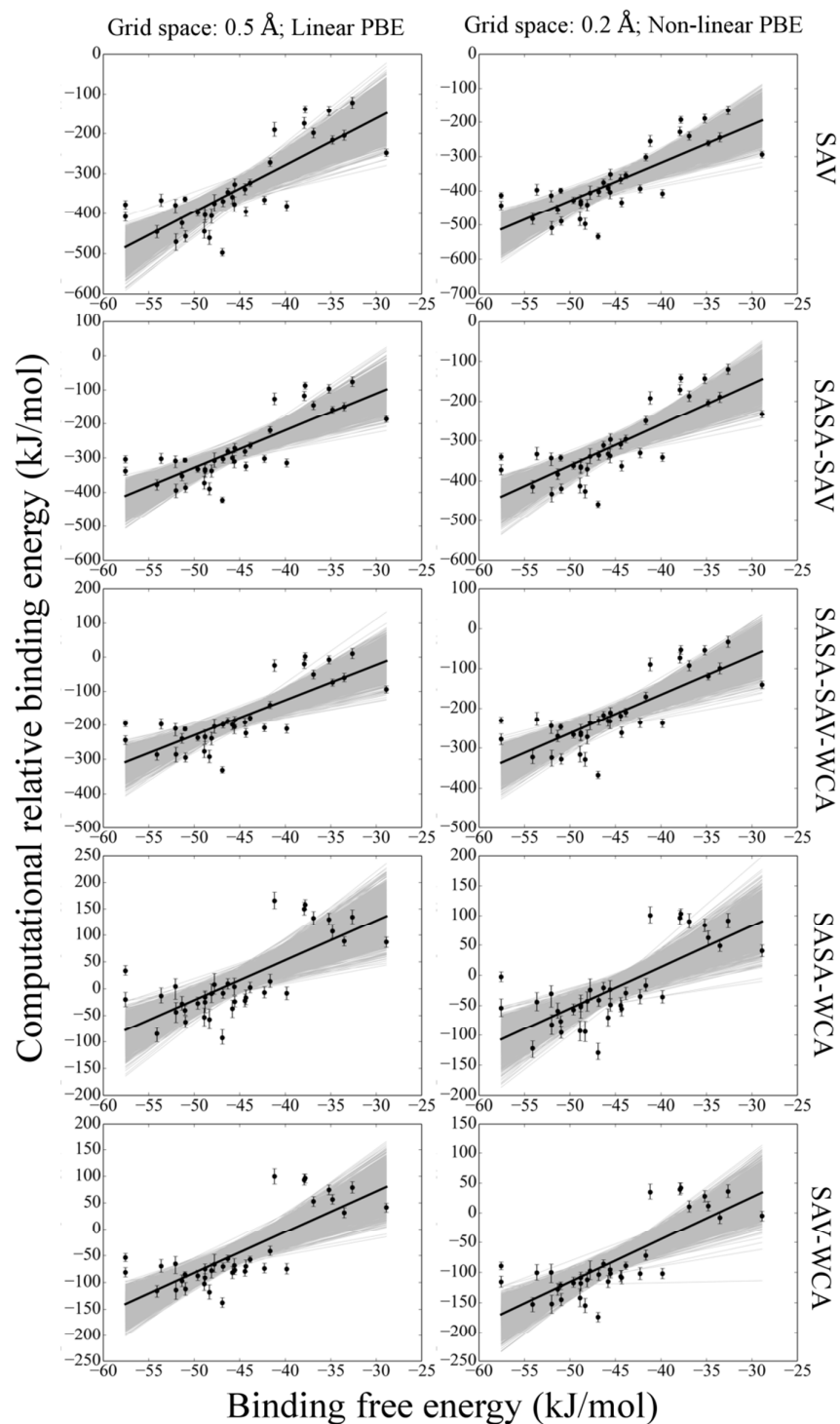


Figure S7: Correlation between experimental binding free energy and calculated binding energy (kJ/mol) with five non-polar solvation models. The dots represent mean of average binding energy after bootstrap and the error bars are 99% confidence interval of mean distribution. Following are the parameters values/choices taken for the G_{polar} : Linear PBE, $\epsilon_{solute} = 2$ and grid resolution of 0.5 Å. (Left panel); Non-linear PBE, $\epsilon_{solute} = 2$ and grid resolution of 0.2 Å (Right panel).

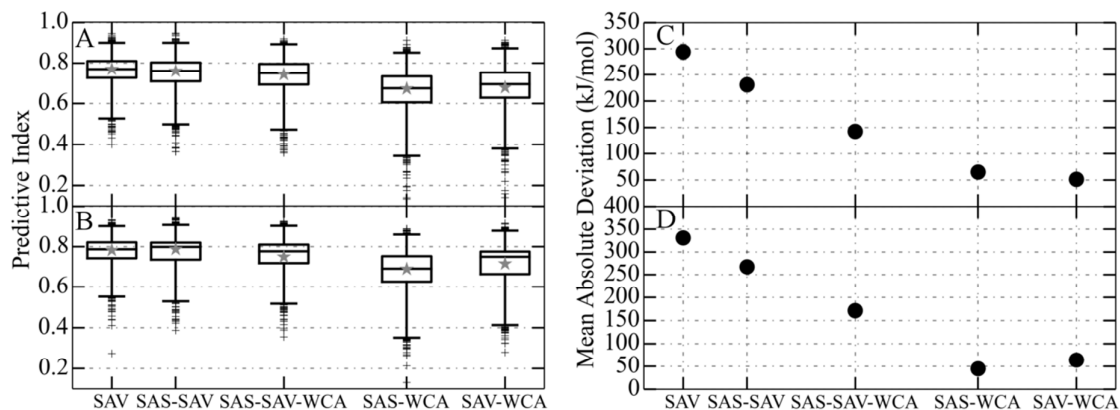


Figure S8: Predictive index (PI) distribution and mean absolute deviation (MAD) for the five different non-polar solvation models. (A-B) for the PI: Box, symbols ('+'), horizontal line shown inside box and asterisk symbols represent the same information as discussed in Figs S5 and are calculated with similar method. (C-D) for the MAD: black dots and error-bar represent average value and standard error, which is calculated using the bootstrap analysis. Following are the parameters values/choices taken for the G_{polar} . (A,C) LPBE, $\epsilon_{solute} = 2$ and 0.5 Å grid resolution. (B,D) NPBE, $\epsilon_{solute} = 2$ and 0.2 Å grid resolution.

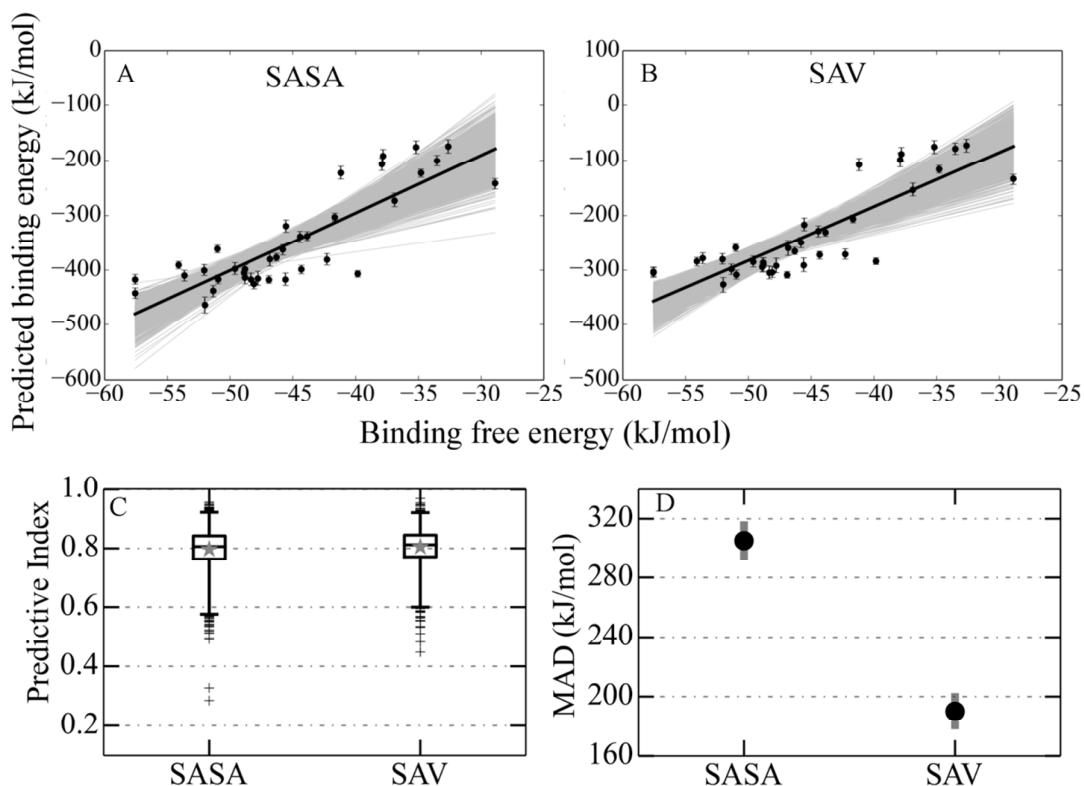


Figure S9: Predicted energy with respect to the experimental energy, predictive index (PI) and mean absolute deviation (MAD) when polar solvation energy was calculated on the grid point spaced by 0.5 \AA , $\epsilon_{\text{solute}} = 2$, bondi radii and using van der Waals (vdW) surface of the solute which is smoothed using the seventh order polynomial function with smoothing window of 0.3 \AA . (A-B) Correlation between experimental and calculated binding energy (kJ/mol). The dots represent mean of average binding energy after bootstrap and the error bars are 99% confidence interval of mean distribution. The plots are shown for non-polar model (A) SASA-only and (B) SAV-only. (C) PI distributions are shown with respect to the two non-polar models. Box, symbols ('+'), horizontal line shown inside box and asterisk symbols represent the similar information as discussed in Figs S5 and are calculated with similar method. (D) MAD values are shown with respect to the two non-polar models. Black dots and error-bar represent average values and standard errors that were calculated using the bootstrap analysis.

REFERENCES

1. Bondi, A., van der Waals Volumes and Radii. *J. Phys. Chem.* **1964**, *68* (3), 441-451.
2. Case, D. A.; Cheatham, T. E.; Darden, T.; Gohlke, H.; Luo, R.; Merz, K. M.; Onufriev, A.; Simmerling, C.; Wang, B.; Woods, R. J., The Amber biomolecular simulation programs. *J. Comput. Chem.* **2005**, *26* (16), 1668-1688.
3. Tsui, V.; Case, D. A., Molecular dynamics simulations of nucleic acids with a generalized born solvation model. *J. Am. Chem. Soc.* **2000**, *122* (11), 2489-2498.
4. Tsui, V.; Case, D. A., Theory and applications of the generalized Born solvation model in macromolecular Simulations. *Biopolymers* **2001**, *56* (4), 275-291.